

# 000 001 002 003 004 005 006 007 008 009 010 011 012 013 014 015 016 017 018 019 020 021 022 023 024 025 026 027 028 029 030 031 032 033 034 035 036 037 038 039 040 041 042 043 044 045 046 047 048 049 050 051 052 053 ADASPEC: ADAPTIVE SPECTRUM FOR ENHANCED NODE DISTINGUISHABILITY

Anonymous authors  
Paper under double-blind review

## ABSTRACT

Spectral Graph Neural Networks (GNNs) achieve strong performance in node classification, yet their node distinguishability remains poorly understood. We analyze how graph matrices and node features jointly influence node distinguishability. Further, we derive a theoretical lower bound on the number of distinguishable nodes, which is governed by two key factors: distinct eigenvalues in the graph matrix and nonzero frequency components of node features in the eigenbasis. Based on these insights, we propose AdaSpec, an adaptive graph matrix generation module that enhances node distinguishability of spectral GNNs without increasing the order of computational complexity. We prove that AdaSpec preserves permutation equivariance, ensuring that reordering the graph nodes results in a corresponding reordering of the node embeddings. Experiments across eighteen benchmark datasets validate AdaSpec’s effectiveness in improving node distinguishability of spectral GNNs.

## 1 INTRODUCTION

Graph Neural Networks (GNNs) have become increasingly popular for graph learning tasks due to their strong performance in tasks such as graph and node classification (Kipf & Welling, 2017; Xu et al., 2019; He et al., 2021; Wang & Zhang, 2022; Qin et al., 2025). Among the various GNN models, spectral GNNs represent a prominent class that transforms graph signals into the spectral domain, enabling graph filters to process information for downstream tasks. Although numerous spectral GNNs have been proposed, their node distinguishability remains insufficiently understood. **Node distinguishability refers to the capacity of a GNN to map topologically or feature-different nodes to different embeddings.** These models typically utilize different graph matrices, such as the normalized adjacency or Laplacian matrix. Further, the distribution of node features across the graph plays a crucial role in model performance (He et al., 2022b; Platonov et al., 2023). To the best of our knowledge, no existing work has systematically analyzed the interaction between the graph matrix and node features in determining node distinguishability in spectral GNNs.

Spectral GNNs with state-of-the-art performance generally follow the form:

$$\Psi(M, X) = g_\Theta(M)f_W(X), \quad (1)$$

where  $M \in \mathbb{R}^{n \times n}$  represents the graph matrix (such as the Laplacian or adjacency matrix),  $X \in \mathbb{R}^{n \times h}$  denotes the node feature matrix,  $g_\Theta(M) = \sum_{k=0}^K \theta_k T_k(M)$  is the graph convolution function parameterized by  $\Theta = \{\theta_k\}_{k=0}^K$ , and  $T_k(\cdot)$  denotes the  $k$ -th polynomial basis. The term  $f_W(X)$  represents the feature transformation function parameterized by  $W$ . Spectral GNNs learn meaningful node features by optimizing  $W$ , projecting them into the spectral domain. By adjusting  $\Theta$ , spectral GNNs filter out unnecessary information and enhance useful information for downstream tasks.

While this formulation illustrates how spectral GNNs process node features through graph convolution, their capacity for node distinguishability remains inadequately understood. This leads to a fundamental question: how does the interaction between the graph matrix  $M$  and the node features  $X$  projected into the spectral domain affect the node distinguishability of spectral GNNs? In this work, we demonstrate that node distinguishability is influenced by the eigenvalue multiplicity and the missing frequency components of node features in the eigenbasis of the graph matrix. Further, we derive a theoretical lower bound on the number of nodes that can be distinguished by spectral GNNs, given a specific graph matrix and node features.

Motivated by our theoretical analysis of node distinguishability, we introduce AdaSpec, an adaptive graph matrix generation module that optimizes the graph matrix to maximize its lower

054 bound on node distinguishability. Designed as a plug-in, AdaSpec can be seamlessly integrated  
 055 into any spectral GNN to enhance node distinguishability. Moreover, spectral GNNs augmented  
 056 with AdaSpec preserve permutation equivariance, ensuring that reordering graph nodes results in a  
 057 corresponding reordering of node embeddings. Finally, AdaSpec maintains the graph’s connectivity,  
 058 guaranteeing that the learned embeddings accurately reflect the underlying graph structure.

059 We evaluate our approach on eighteen benchmark node classification datasets, covering a range  
 060 of small- and large-scale graphs with both homophilic and heterophilic structures in Section 6.  
 061 Spectral GNNs with AdaSpec achieve notable performance improvements on heterophilic graphs,  
 062 while maintaining or slightly improving accuracy on homophilic ones. These results validate the  
 063 effectiveness of AdaSpec in boosting node distinguishability. Additionally, experimental results show  
 064 that the order of time complexity of spectral GNNs with and without AdaSpec are the same.

## 066 2 RELATED WORKS

068 **Spectral GNNs.** Spectral GNNs perform graph convolution by applying filters in the spectral  
 069 domain for representation learning. Based on the design of their graph filters, spectral GNNs can be  
 070 categorized into polynomial (He et al., 2022a; 2021) and rational types (Levie et al., 2019; Bianchi  
 071 et al., 2021; Li et al., 2025). Polynomial graph filters are computationally efficient and localized in the  
 072 vertex domain (Hammond et al., 2009; Defferrard et al., 2016), and this paper focuses on their analysis.  
 073 Recent studies primarily investigate how different polynomial bases affect spectral GNN performance,  
 074 for instance, ChebNet, ChebNetII, JacobiConv, BernNet, GPRGNN and GLN (Defferrard et al.,  
 075 2016; He et al., 2022a; Wang & Zhang, 2022; He et al., 2021; Chien et al., 2021; Li & Wang, 2024).  
 076 Further, FavardGNN, UniFilter and PolyCF learn polynomial bases that adapt to different graph  
 077 structures (Guo & Wei, 2023; Huang et al., 2024; Qin et al., 2025).

078 Above spectral GNNs use fixed graph matrices like normalized adjacency or Laplacian matrices.  
 079 While research has focused on effect of polynomial bases on performance of spectral GNNs, we  
 080 demonstrate the critical role of the graph matrix. We analyze how the interaction between the graph  
 081 matrix and node features affects spectral GNN performance. Further, we propose AdaSpec, a graph  
 082 matrix generation module to enhance the performance of spectral GNNs.

083 **Expressive Power of Spectral GNNs.** The expressive power of GNNs in graph classification has  
 084 been extensively analyzed through the Weisfeiler-Lehman (WL) test (Li & Leskovec, 2022; Zhang  
 085 et al., 2023; Jin et al., 2025), which are algorithms determining graph isomorphism (Weisfeiler  
 086 & Leman, 1968). In contrast, the expressive power of GNNs for node classification remains less  
 087 explored. The expressive capacity of linear spectral GNNs has been analyzed via the uniform  
 088 approximation theorem in (Wang & Zhang, 2022), which shows that when the graph matrix has no  
 089 repeated eigenvalues and node features span all frequency components, the model can approximate  
 090 any one-dimensional function. However, these conditions rarely hold in real-world graphs, where  
 091 symmetric structures are common and node features are often sparse. An eigenvalue correction  
 092 method was proposed in (Lu et al., 2024) to enhance the expressiveness of spectral GNNs. **This**  
 093 **method reassigns eigenvalues purely by their sorted index, it does not preserve eigenspaces under**  
 094 **node permutations, thereby breaking permutation equivariance**, which is theoretically unsound.

095 Our work investigates the expressive power of spectral GNNs from the perspective of node  
 096 distinguishability. We extend the understanding of how the interaction between the graph matrix  
 097 and node features influences node distinguishability in spectral GNNs. Notably, our analysis goes  
 098 beyond linear GNNs by incorporating nonlinear feature transformations  $f_W$ . Moreover, we rigorously  
 099 establish a theoretical lower bound on the number of distinguishable nodes in spectral GNNs.

100 **Graph Rewiring.** Another line of research focuses on improving the performance of GNNs through  
 101 graph rewiring techniques, which modify the graph topology. Early methods include DropEdge  
 102 and EDGEWIRE, which randomly or uses degree-preserving strategy to remove edges to alleviate  
 103 over-smoothing (Rong et al., 2020; Chan & Akoglu, 2016). Curvature-based approaches (Topping  
 104 et al., 2022) adjust connectivity using discrete Ricci curvature to combat over-squashing, while  
 105 locality-aware strategies preserve structures efficiency (Barbero et al., 2024). More recent methods  
 106 include DiffWire, a differentiable and parameter-free approach guided by the Lovász bound (Arnaiz-  
 107 Rodríguez et al., 2022); FoSR, which improves spectral expansion (Karhadkar et al., 2023); and  
 108 GPER, selecting edges based on effective resistance to enhance information flow (Shen et al., 2024).

108 While graph rewiring methods offer valuable insights into improving GNN performance, their  
 109 objectives and underlying mechanisms differ fundamentally from ours. Graph rewiring addresses  
 110 structural issues by modifying graph topology in the spatial domain as a preprocessing step. In  
 111 contrast, our method enhances node distinguishability in the spectral domain through an adaptive  
 112 graph matrix generation module that trains end-to-end with spectral GNNs.  
 113

### 114 3 PRELIMINARIES

116 Let  $G = (\mathcal{V}, \mathcal{E}, X)$  denote an undirected, simple graph, where  $\mathcal{V}$  is the set of nodes with cardinality  
 117  $|\mathcal{V}| = n$ ,  $\mathcal{E}$  is the set of edges, and  $X \in \mathbb{R}^{n \times h}$  is the node feature matrix. For each node  $v \in \mathcal{V}$ ,  
 118  $X(v) \in \mathbb{R}^h$  denotes its associated feature vector. The graph structure is represented by the adjacency  
 119 matrix  $A \in \{0, 1\}^{n \times n}$ , where  $A_{ij} = 1$  if  $(v_i, v_j) \in \mathcal{E}$ , and 0 otherwise. The degree matrix  
 120  $D \in \mathbb{R}^{n \times n}$  is diagonal with entries  $D_{ii}$  equal to the degree of node  $v_i$ . The normalized adjacency  
 121 matrix is defined as  $\tilde{A} = D^{-\frac{1}{2}} A D^{-\frac{1}{2}}$ . The normalized graph Laplacian is given by  $\tilde{L} = I - \tilde{A}$ ,  
 122 where  $I \in \mathbb{R}^{n \times n}$  is the identity matrix.  
 123

123 Two nodes  $u$  and  $v$  in an undirected graph  $G$  are *structurally equivalent*  $s_u \sim s_v$  if they share  
 124 exactly the same neighbors; formally, for every other node  $w \in \mathcal{V} \setminus \{u, v\}$ ,  $(u, w) \in \mathcal{E} \iff (v, w) \in \mathcal{E}$ . In effect, swapping  $u$  and  $v$  leaves the graph's adjacency relation unchanged.  
 125

126 A *permutation* of the node set  $\mathcal{V}$  is a bijection  $\pi : \mathcal{V} \rightarrow \mathcal{V}$ . The set of all permutations on  $\mathcal{V}$   
 127 forms the symmetric group  $\text{Sym}(\mathcal{V})$ . An *automorphism* of the graph  $G$  is a permutation  $\pi \in \text{Sym}(\mathcal{V})$   
 128 satisfying the following conditions: (1) edge preservation:  $(v, u) \in \mathcal{E} \iff (\pi(v), \pi(u)) \in \mathcal{E}$ ,  
 129  $\forall v, u \in \mathcal{V}$ , and (2) feature preservation:  $X(\pi(v)) = X(v)$ ,  $\forall v \in \mathcal{V}$ . The *automorphism group*  
 130 of  $G$ , denoted  $\text{Aut}(G)$ , is the set of all such automorphisms.  
 131

131 Two nodes  $u$  and  $v$  are said to be *isomorphic*, denoted  $u \sim v$ , if they belong to the same orbit  
 132 under  $\text{Aut}(G)$ ; that is, there exists a permutation  $\pi \in \text{Aut}(G)$  such that  $\pi(v) = u$ . Otherwise,  $u$  and  
 133  $v$  are *non-isomorphic*.

134 An important property of functions defined on graphs is *permutation equivariance*, which ensures  
 135 that the output remains consistent under any reordering of the nodes. Formally,

136 **Definition 3.1** (Permutation Equivariance). Let  $\mathcal{G}$  denote the set of graphs. A function  $f : \mathcal{G} \rightarrow \mathbb{R}^{n \times d}$   
 137 is said to be *permutation equivariant* if, for any graph  $G \in \mathcal{G}$  and any permutation  $\pi \in \text{Sym}(\mathcal{V})$ , it  
 138 holds that

$$139 \quad f(\pi(G)) = \pi(f(G)),$$

140 where  $\pi(G)$  denotes the graph obtained by permuting the nodes of  $G$  according to  $\pi$ , and  $\pi(f(G))$   
 141 denotes the corresponding permutation of the output of  $f$ .  
 142

### 143 4 NODE DISTINGUISHABILITY OF SPECTRAL GNNs

144 The node distinguishability of a spectral GNN refers to its ability to distinguish non-isomorphic  
 145 nodes within graphs. Formally,

146 **Definition 4.1** (Node Distinguishability). For a spectral GNN with function class  $\mathcal{F}$ , where each  
 147  $f \in \mathcal{F} : \mathcal{G} \rightarrow \mathbb{R}^{n \times d}$  maps a graph to node representations, node distinguishability refers to the ability  
 148 to learn a function that assigns distinct representations to non-isomorphic nodes:  
 149

$$150 \quad f(G)_v \neq f(G)_u \quad \text{for all } v, u \in \mathcal{V} \text{ where } v \not\sim u$$

151 where  $f(G)_v$  and  $f(G)_u$  denote representations of node  $v$  and  $u$ .  $v \not\sim u$  indicates node  $u, v$  are  
 152 non-isomorphic.  
 153

154 The spectral GNN's node distinguishability capacity that mapping non-isomorphic nodes to  
 155 distinct representations is fundamentally determined by its function class  $\mathcal{F}$ . To understand how  
 156 spectral GNNs of the form given in Equation (1) distinguish nodes, whose input consists of a graph  
 157 matrix  $M$  and a feature matrix  $X$ , we begin by formally defining the spectrum of  $M$  and the frequency  
 158 components of  $X$ .

159 **Definition 4.2** (Spectrum and Frequency Components). Let  $M = U \Lambda U^\top$  be the eigendecomposition  
 160 of a graph matrix  $M \in \mathbb{R}^{n \times n}$ , where  $\Lambda$  is a diagonal matrix of eigenvalues and  $U = [u_1, \dots, u_n]$   
 161 contains the corresponding eigenvectors. The *spectrum* of  $M$ , denoted  $\text{spec}(M)$ , is the multiset  
 162 of eigenvalues:  $\text{spec}(M) = \{\{\lambda_1, \lambda_2, \dots, \lambda_n\}\}$ , where  $\lambda_i = \Lambda_{ii}$ . Let  $\text{support}(\text{spec}(M))$  be

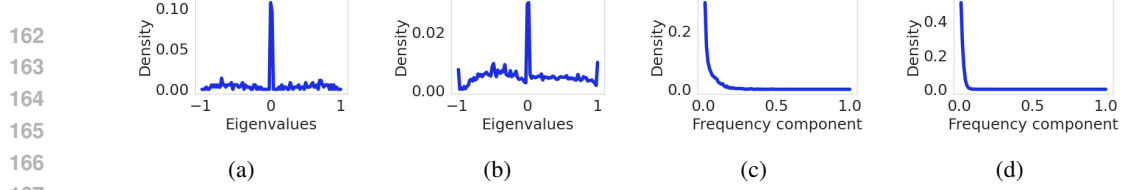


Figure 2: Eigenvalues and frequency component distributions.

the underlying set of  $\text{spec}(M)$ . Define  $d_M = |\text{supp}(\text{spec}(M))|$ , which is the number of distinct eigenvalues. Given node features  $X \in \mathbb{R}^{n \times h}$ , the frequency components in the eigenbasis of  $M$  are  $\tilde{X} = U^\top X$ , where  $\tilde{X}_i = u_i^\top X$  is the  $i$ -th frequency component. The number of non-zero frequency components is  $\|\tilde{X}^{(M)}\|_0 = |\{\tilde{X}_i \mid \tilde{X}_i \neq 0_h\}|$ .

The limitations of node distinguishability in spectral GNNs stem from two key factors: Eigenvalue multiplicity of the graph matrix  $M$  and the missing of frequency components of node features  $X$  when projected onto the eigenbasis of  $M$ . In Figure 1, we show that spectral GNNs with a first-order polynomial filter and normalized adjacency matrix  $\tilde{A}$  as graph matrix cannot distinguish node 1 and 3. (1) Non-distinguishable nodes can exist when there are missing frequency components that  $d_{\tilde{A}} = 5 = n$  but  $\|X^{(\tilde{A})}\|_0 = 3 < n$  in Figure 1(a). (2) Non-distinguishable nodes can exist when there are repeated eigenvalues  $d_{\tilde{A}} = 3 < n$  even if  $\|X^{(\tilde{A})}\|_0 = 5 = n$  in Figure 1(b). Nodes 1 and 3 in both subfigures are non-isomorphic but spectral GNNs yield identical embeddings for them. Hence they are indistinguishable. We provide a theoretical bound on the number of nodes that can be distinguished by spectral GNNs, stated as follows.

**Theorem 4.3.** *For  $X \neq 0_{n \times n}$ , there exist a spectral GNN  $\Psi(M, X)$  that can distinguish at least  $\min(d_M, \|\tilde{X}^{(M)}\|_0)$  nodes on graph.*

This result provides a fundamental guarantee on the node distinguishability of spectral GNNs. The lower bound depends on both the number of distinct eigenvalues  $d_M$  and the number of non-zero frequency components  $\|\tilde{X}^{(M)}\|_0$ , which together characterize the alignment between the graph matrix  $M$  and the node features  $X$ . When multiple eigenvectors share the same eigenvalue, the graph filter  $g_\Theta$  applies identical transformations to them, preventing from distinguishing different structural patterns. Similarly, if node features lack frequency components corresponding to certain eigenvectors, structural differences captured by those eigenvectors become invisible in embeddings. This has practical implications: increasing distinct eigenvalue number  $d_M$  and non-zero frequency components of  $X$  in the eigenbasis of  $M$  improves the theoretical guarantee on the lower bound of number of distinguishable nodes, offering a clear direction for enhancing the expressive power of spectral GNNs.

In real-world graphs, we observe that eigenvalue multiplicity and missing frequency component are very common.

**Observation I** (Eigenvalues of Multiplicity.) The normalized graph adjacency matrix  $\tilde{A} = D^{-1/2}AD^{-1/2}$  often contains eigenvalues with multiplicities greater than one and the eigenvalue zero has largest multiplicity.

We illustrate the eigenvalue distribution of the normalized graph adjacency matrix for the Texas and Cora datasets in Figure 2(a-b). Additional eigenvalue distributions for various other real-world datasets are provided in Figure 3 (Appendix). This phenomenon is also observed in (Lim et al., 2023). Graph symmetry, repeated substructures often lead to repeated eigenvalues in the normalized adjacency matrix and reduce its rank. Real-world graphs also tend to be sparse due to many low-degree nodes, further lowering the rank. Since the rank of a real symmetric matrix equals the number of non-zero eigenvalues, low-rank matrices imply high multiplicity of the zero eigenvalue.

Node features in connected real-world graphs are sampled independently of the graph structure. For instance, in citation networks (such as Cora and PubMed), node features are the textual content of

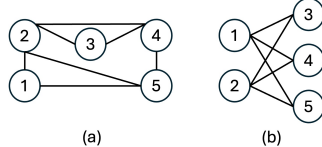


Figure 1: Nodes 1 and 3 cannot be distinguished by spectral GNNs of  $K = 1$  with  $\tilde{A}$ . (a) Missing frequency components:  $X = [1, 0, 1, -1, -1]$ ,  $d_{\tilde{A}} = 5$ ,  $\|X^{(\tilde{A})}\|_0 = 3$ . (b) Eigenvalue multiplicity:  $X = [1, 0, 1, 1, -1]$ ,  $d_{\tilde{A}} = 3$ ,  $\|X^{(\tilde{A})}\|_0 = 5$ .

216 papers, which are collected independently of the graph structure. Thus, graph signals are not aligned  
 217 with the graph's eigenvectors. We have below observations.

218 **Observation II** (Missing Frequency Components.) Many frequency components of graph signal  
 219 (node feature) is zero in the eigenbasis of normalized graph adjacency matrix  $\tilde{A}$ .

220 We illustrate the distribution of frequency components for Texas and Cora in Figure 2(c-d), where  
 221 most components are zero. Additional results for other real-world datasets are provided in Figure 4  
 222 (Appendix). Zero frequency component means that the frequency component in the direction of  
 223 corresponding eigenvectors is missing. Real-world node features are often either smooth or oscillatory,  
 224 containing only low or high-frequency components, leading to many others to be zero or negligible.  
 225 Additionally, features are typically sparse, with only  $k$  non-zero entries that  $k \ll n$ . When projected  
 226 onto the eigenbasis, each component scales as  $O(k/\sqrt{n})$ . As  $n \rightarrow \infty$ , the proportion of non-zero  
 227 frequency components tends toward zero.

228 Based on above observations and Theorem 4.3, we propose AdaSpec to enhance the node  
 229 distinguishability of spectral GNNs.

## 231 5 ADASPEC

233 AdaSpec generates a graph matrix that adapts to both the graph structure and node features, enabling  
 234 it to serve as a plug-in module for any spectral GNN  $\Psi(M, X)$  of the form in Equation (1). The  
 235 spectral GNN augmented with AdaSpec is defined as:

$$236 \quad \Psi^+(A, X) = g_\Theta(\Omega(A, X))f_W(X), \quad (2)$$

237 where  $\Omega$  maps the adjacency matrix  $A$  and node features  $X$  to a new graph matrix. The functions  $g_\Theta$   
 238 and  $f_W(X)$  remain the same as those in  $\Psi(M, X)$ .

239 AdaSpec enables  $\Psi^+(A, X)$  to capture richer interactions between graph structure and node  
 240 features, which are not possible using fixed matrices in classic spectral GNNs  $\Psi(M, X)$ . To ensure  
 241 permutation equivariance of node embeddings, the generated graph matrix  $M = \Omega(A, X)$  must  
 242 satisfy two key properties: (1)  $M$  commutes with  $\text{Aut}(G)$ :  $P_\sigma M = MP_\sigma, \forall \sigma \in \text{Aut}(G)$  where  $P_\sigma$   
 243 is the permutation matrix corresponding to the automorphism  $\sigma$ ; (2)  $M$  preserves edge connectivity:  
 244  $M_{ij} \neq 0 \Leftrightarrow e_{ij} \in \mathcal{E}$  and  $M_{ij} = 0 \Leftrightarrow e_{ij} \notin \mathcal{E}$ . Thus, we design  $\Omega(A, X)$  as

$$245 \quad \Omega(A, X) = \Omega_D(A) + \alpha_1 \Omega_S(A) + \alpha_2 \Omega_F(X) \quad (3)$$

246 where  $\Omega_D(A)$  is designed to increase the number of distinct eigenvalues,  $\Omega_S(A)$  aims to reduce the  
 247 multiplicity of zero eigenvalues, and  $\Omega_F(X)$  is designed to decrease missing frequency components  
 248 of  $X$ . The hyperparameters  $\alpha_1, \alpha_2$  control the eigenvalue range for stable training.

### 250 5.1 INCREASE DISTINCT EIGENVALUES

252 According to Theorem 4.3, increasing the number of distinct eigenvalues of the graph matrix can  
 253 raise the lower bound of number of nodes distinguished by a spectral GNN, thereby increasing its  
 254 node distinguishability. To achieve this, the term  $\Omega_D(A)$  in AdaSpec is designed as follows:

$$255 \quad \Omega_D(A) = (D + B)^{-1/2} (A + B) (D + B)^{-1/2},$$

256 where  $A$  and  $D$  are the graph adjacency matrix and the degree matrix, respectively, and  $B = \text{diag}(b)$   
 257 is a learnable diagonal matrix with non-negative elements.

258 The diagonal element of  $B$  is initialized as  $b_u = 1/D_{uu}$ , ensuring nodes with the same degree  
 259 start with the same bias. For isomorphic nodes  $u \sim v$ , we have  $b_u = b_v$  throughout training; for  
 260  $u \not\sim v$ , training yields  $b_u \neq b_v$ . This initialization preserves permutation equivariance of  $\Psi^+(A, X)$ ,  
 261 as shown in Proposition 5.5. Adding  $B$  to  $A$  introduces node-specific flexibility, enabling  $A + B$  and  
 262  $D + B$  to adapt to graphs. This enhances node distinguishability by allowing structurally equivalent  
 263 but feature different nodes to play distinct roles. For two non-isomorphic nodes  $u, v$  that  $u \not\sim v$ , if  
 264  $s_u \sim s_v$  but  $X(u) \neq X(v)$ , introducing different biases  $b_u \neq b_v$  breaks structure symmetry and  
 265 reduces eigenvalue multiplicity. Intuitively,  $B$  modifies the self-loop strength, altering information  
 266 flow from the node itself. We later provide theoretical justification that this increases the number of  
 267 distinct eigenvalues.

268 **Theorem 5.1** (Increased Distinct Eigenvalues). *Given a graph  $G$  with the adjacency matrix  $A$ , and  
 269 the degree matrix  $D$ , we have:*

$$d_{\Omega_D(A)} \geq d_{\tilde{A}}$$

270 We prove that for any  $A$ , there exist a diagonal matrix  $B$  so that  $\Omega_D(A)$  has  $n$  distinct eigenvalues.  
 271 This indicates that the lower bound of the number of distinguishable nodes for spectral GNNs using  
 272  $\Omega_D$  is greater than or equal to that for those using  $\tilde{A}$ , according to Theorem 4.3.  
 273

## 274 5.2 SHIFTS EIGENVALUES FROM ZERO

275 The presence of zero eigenvalues forces spectral filters to suppress the associated frequency components,  
 276 thereby hindering node distinguishability. We shift eigenvalues away from zero by using:  
 277

$$278 \Omega_S(A) = I.$$

279 We choose the identity matrix because adding it to any matrix shifts the eigenvalues while preserving  
 280 the eigenvectors. This ensures minimal alteration to the original matrix.

281 Adding term  $\epsilon\Omega_S$  to any matrix  $C$  can reduce the number of zero eigenvalues. As all eigenvalues  
 282 of  $C$  add the same scalar  $\epsilon$ , distinct eigenvalues remain distinct after addition. As all eigenvectors of  
 283  $C$  stays the same, so the number of non-zero frequency component of node feature stays the same.

## 284 5.3 INCREASE FREQUENCY COMPONENTS

285 We can increase the number of non-zero frequency component to the node distinguishability of  
 286 spectral GNNs. Given a node feature matrix  $X$ , we design a matrix  $\Omega_F$  that adapts to  $X$  to increase  
 287 the frequency components:

$$288 \Omega_F(X) = \sum_{i=1}^h \frac{X_{:i} X_{:i}^\top}{\|X_{:i}\|_F^2} \circ A \quad (4)$$

289 where  $\circ$  denotes the Hadamard product.

290 By dividing by the Frobenius norm  $\|X_{:i}\|_F^2$ , features with larger magnitudes don't dominate the  
 291 transformation. We prove in theory that for any symmetric matrix  $C$  of no repeated eigenvalues,  
 292 adding  $\epsilon\Omega_F(X)$  can increase non-zero frequency components.

293 **Theorem 5.2** (Non-Decreasing Frequency Components). *For a real symmetric matrix  $C \in \mathbb{R}^{n \times n}$  of  
 294 no repeated eigenvalues with orthonormal basis  $\{u_r\}_{r \in [n]}$ . Under Condition 5.3, the following holds  
 295 for index  $i \in [h]$ :*

$$296 \|\tilde{X}_{:i}^{(C+\epsilon\Omega_F)}\|_0 > \|\tilde{X}_{:i}^{(C)}\|_0$$

297 where  $\epsilon$  is a non-zero constant.

298 **Condition 5.3** (Non-zero feature projections). Let  $C \in \mathbb{R}^{n \times n}$  be a real symmetric matrix with  
 299 orthonormal eigenbasis  $\{u_r\}_{r=1}^n$ . There exist two column node feature vectors  $X_{:i}$  and  $X_{:l}$  with  
 300  $i, l \in [h]$  and  $i \neq l$  such that  $u_k^\top X_{:i} \neq 0$ ,  $u_k^\top X_{:l} \neq 0$ , and  $u_j^\top X_{:l} \neq 0$  for some indices  $k, j \in [n]$ .

301 Condition 5.3 are naturally satisfied in most real-world graph datasets. This condition requires  
 302 that node features have non-zero projections onto certain eigenvectors of the graph matrix. Natural  
 303 heterogeneity in node features makes it likely that different nodes will have diverse nonzero  
 304 projections onto eigenvectors, even with sparse features. Additionally, while feature correlation  
 305 exists, real-world graph typically varies a lot along certain dimensions, satisfying our non-zero  
 306 projection condition. Therefore, incorporating  $\Omega_F(X)$  ensures that the number of non-zero frequency  
 307 components of node features is increased in real-world graphs.

308 In summary, each component of  $\Omega(A, X)$  either increases the number of distinct eigenvalues or  
 309 the number of non-zero frequency components of the node features in the eigenbasis of the graph  
 310 matrix. By Theorem 4.3, this leads to a higher lower bound on the number of distinguishable nodes,  
 311 thereby enhancing node distinguishability. We show properties of our design  $\Omega(A, X)$  as below.

312 **Theorem 5.4.** *For a graph  $G$ , the learnable matrix  $\Omega(A, X)$  is commutative with  $\text{Aut}(G)$  and  
 313 preserves edge connectivity.*

314 As  $\Omega(A, X)$  satisfies desirable properties, it ensures that the augmented spectral GNNs  $\Psi^+(A, X)$   
 315 with AdaSpec remains permutation equivariant.

316 **Proposition 5.5.** *When  $f_W$  is permutation equivariant, spectral GNNs  $\Psi^+(A, X)$  augmented with  
 317 AdaSpec is permutation equivariant.*

318 Theorem 5.4 and Proposition 5.5 ensures that for spectral GNNs  $\Psi^+(A, X)$ , reordering the graph  
 319 nodes results in a corresponding reordering of node embeddings. AdaSpec can be combined with any  
 320 spectral GNNs to enhance their node distinguishability.

324 5.4 TIME COMPLEXITY ANALYSIS  
325

326 The time complexity of classic spectral GNNs  $\Psi(M, X)$  and  $\Psi^+(A, X)$  augmented with AdaSpec is  
327 in the same order in both forward and backward propagation.  $\Omega_F(X)$  in AdaSpec will increase the  
328 pre-computing time, but it needs to be computed only once. We list the time complexity in Table 1.

329 The time complexity can be analyzed in two main phases: pre-computation and forward/backward  
330 propagation. During pre-computation, graph matrix normalization requires  $O(|\mathcal{V}| + |\mathcal{E}|)$  operations  
331 such as graph adjacency matrix normalization.  $\Omega_F(X)$  in  $\Psi^+(A, X)$  requires an additional  $O(h(|\mathcal{V}| +$   
332  $|\mathcal{E}|))$  where computation is efficiently limited to non-zero entries in the adjacency matrix. Thus, the  
333 one-off pre-computing of  $\Psi^+(A, X)$  scales linearly in the size of graph and node feature dimension.

334 For forward and backward propagation, the feature transformation step  $f_W(X)$  incurs a com-  
335 plexity of  $O(|W|h)$ , while graph convolution  $g_\Theta$  requires  $O(KT|\mathcal{E}|)$  operations when  $T_k(M)$  is  
336 computed recursively, such as in ChebNet, JacobiConv. Although  $\Psi^+(A, X)$  requires additional  
337 computation of  $\Omega(A, X)$  during each forward pass and gradient calculation for matrix  $B$  during  
338 backpropagation at a cost of  $O(|\mathcal{V}| + |\mathcal{E}|)$ , this does not change the overall asymptotic complexity.

339 6 EXPERIMENTS  
340

341 We design our experiments to investigate the following research questions: (1) **Q1**: To what extent  
342 does AdaSpec generate task-adaptive graph matrices that enhance node distinguishability in spectral  
343 GNNs? (2) **Q2**: What is the contribution of each component within AdaSpec to overall performance?  
344 (3) **Q3**: How does AdaSpec affect the spectral properties of the graph matrix, particularly in terms  
345 of increasing the number of distinct eigenvalues? (4) **Q4**: What is the computational overhead  
346 introduced by integrating AdaSpec into spectral GNNs during training?

347 **Experimental Setup.** We conduct experiments on eighteen benchmark datasets for node classifica-  
348 tion to verify the effectiveness of AdaSpec. Datasets includes: six small heterophilic graphs (Texas,  
349 Wisconsin, Actor, Chameleon, Squirrel, Cornell), five large heterophilic graphs (Roman\_Empire,  
350 Amazon\_Ratings, Minesweeper, Tolokers, Questions) and seven homophilic graphs (Citeseer,  
351 Pubmed, Cora, Computers, Photo, Coauthor-CS, Coauthor-Physics). Statistics of datasets, details  
352 about the baselines, and the setting of hyperparameters are included in Appendix B. For each dataset,  
353 we follow (Chien et al., 2021; He et al., 2022a) and use sparse splitting that nodes are randomly  
354 divided into training/validation/testing with ratios of 2.5%/2.5%/95%, respectively. Notably, for  
355 Citeseer, Pubmed, and Cora datasets, 20 nodes per class are for training, 500 nodes for validation,  
356 and 1,000 nodes for testing.

357 We chose five popular spectral GNNs as our baselines: ChebNet (Defferrard et al., 2016),  
358 GPRGNN (Chien et al., 2021), BernNet (He et al., 2021), JacobiConv (Wang & Zhang, 2022), and  
359 ChebNetII (He et al., 2022a), and compare their performances augmented with AdaSpec and with  
360 fixed graph matrix across all datasets. For each spectral GNN, we use GNN (O) to denote the original  
361 model and GNN (M) to denote the spectral GNNs augmented by AdaSpec, with  $\Delta \uparrow$  indicating the  
362 performance improvement.

363 **Effectiveness of AdaSpec.** We present the node classification performance with and without the  
364 AdaSpec on all small heterophilic datasets and a subset of large heterophilic datasets in Table 2.  
365 The Minesweeper and Question datasets are particularly challenging to classify, as their label  
366 informativeness (i.e., the mutual information between the labels of the central node and its neighbors)  
367 is zero (Platonov et al., 2023). The complete experimental results are in Table 9 (Appendix). Results  
368 on homophilic graphs are shown in Table 3 .

Spectral GNNs	Parameter Count	Pre-computing Complexity	Forward/Backward Complexity
$\Psi(M, X)$	$1 + K$	$O( \mathcal{V}  +  \mathcal{E} )$	$O(KT \mathcal{E}  +  \mathcal{V}  W )$
$\Psi^+(A, X)$	$1 + K +  \mathcal{V} $	$O(h( \mathcal{V}  +  \mathcal{E} ))$	$O(KT \mathcal{E}  +  \mathcal{V}  W )$

375 Table 1: Time complexity comparison of GNNs with and without AdaSpec.  $\mathcal{V}$  and  $\mathcal{E}$  denotes the  
376 node and edge set respectively.  $h$  is the node feature dimension.  $T$  is the node class number.  $K$  is the  
377 polynomial order of spectral GNNs.

Model	Texas	Wisconsin	Actor	Chameleon	Squirrel	Cornell	Minesweeper	Questions
ChebNet(O)	38.67 $\pm$ 9.31	32.92 $\pm$ 7.38	25.15 $\pm$ 0.69	29.32 $\pm$ 4.13	24.23 $\pm$ 3.24	31.33 $\pm$ 7.51	86.29 $\pm$ 0.2	55.13 $\pm$ 0.54
ChebNet(M)	51.16 $\pm$ 8.56	33.83 $\pm$ 9.38	25.38 $\pm$ 0.67	29.73 $\pm$ 3.3	23.2 $\pm$ 3.94	33.47 $\pm$ 7.92	86.7 $\pm$ 0.23	55.2 $\pm$ 1.52
$\Delta \uparrow$	<b>+12.49</b>	<b>+0.91</b>	<b>+0.23</b>	<b>+0.41</b>	-1.03	<b>+2.14</b>	<b>+0.41</b>	<b>+0.07</b>
ChebNetII(O)	56.24 $\pm$ 1.39	51.5 $\pm$ 5.63	29.89 $\pm$ 0.68	35.26 $\pm$ 3.66	37.19 $\pm$ 0.66	39.54 $\pm$ 6.88	78.35 $\pm$ 0.14	64.13 $\pm$ 0.95
ChebNetII(M)	56.76 $\pm$ 3.12	52.0 $\pm$ 7.75	30.43 $\pm$ 1.23	35.62 $\pm$ 3.52	36.88 $\pm$ 0.69	39.94 $\pm$ 7.05	79.1 $\pm$ 0.09	65.54 $\pm$ 0.7
$\Delta \uparrow$	<b>+0.52</b>	<b>+0.5</b>	<b>+0.54</b>	<b>+0.36</b>	-0.31	<b>+0.4</b>	<b>+0.75</b>	<b>+1.41</b>
JacobiConv(O)	55.09 $\pm$ 5.95	49.0 $\pm$ 10.51	32.15 $\pm$ 0.77	34.29 $\pm$ 3.82	29.29 $\pm$ 1.99	38.96 $\pm$ 8.79	87.34 $\pm$ 0.12	64.72 $\pm$ 0.38
JacobiConv(M)	57.43 $\pm$ 3.93	52.33 $\pm$ 8.88	32.52 $\pm$ 0.75	38.16 $\pm$ 1.18	31.35 $\pm$ 1.68	41.62 $\pm$ 10.06	89.13 $\pm$ 0.1	65.8 $\pm$ 0.18
$\Delta \uparrow$	<b>+2.31</b>	<b>+3.33</b>	<b>+0.37</b>	<b>+3.87</b>	<b>+2.06</b>	<b>+2.66</b>	<b>+1.79</b>	<b>+1.08</b>
GPRGNN(O)	48.15 $\pm$ 4.74	44.25 $\pm$ 5.92	30.39 $\pm$ 1.24	32.5 $\pm$ 2.92	27.7 $\pm$ 3.88	34.39 $\pm$ 6.88	87.15 $\pm$ 0.49	53.14 $\pm$ 0.27
GPRGNN(M)	58.27 $\pm$ 4.97	53.25 $\pm$ 7.21	30.4 $\pm$ 1.51	32.82 $\pm$ 4.76	27.3 $\pm$ 6.03 $\pm$ 4.77	36.13 $\pm$ 7.52	88.58 $\pm$ 0.18	58.19 $\pm$ 0.36
$\Delta \uparrow$	<b>+10.12</b>	<b>+9.0</b>	<b>+0.01</b>	<b>+0.32</b>	-0.4	<b>+1.74</b>	<b>+1.43</b>	<b>+5.05</b>
BernNet(O)	56.19 $\pm$ 7.52	49.38 $\pm$ 5.75	30.5 $\pm$ 1.18	35.35 $\pm$ 3.46	33.41 $\pm$ 3.42	36.82 $\pm$ 10.64	76.54 $\pm$ 0.23	64.86 $\pm$ 0.37
BernNet(M)	58.9 $\pm$ 4.11	51.96 $\pm$ 7.84	30.61 $\pm$ 0.67	39.61 $\pm$ 1.55	34.46 $\pm$ 3.52	40.23 $\pm$ 5.66	76.95 $\pm$ 0.21	65.2 $\pm$ 0.31
$\Delta \uparrow$	<b>+2.71</b>	<b>+2.58</b>	<b>+0.11</b>	<b>+4.26</b>	<b>+1.05</b>	<b>+3.41</b>	<b>+0.41</b>	<b>+0.34</b>

Table 2: Performance of spectral GNNs with/without AdaSpec on heterophilic datasets. ROC AUC is reported on Minesweeper, Questions. Testing accuracy is reported on other datasets. High accuracy and ROC AUC indicate good performance.

Model	Citeseer	Pubmed	Cora	Computers	Photo	Coauthor-CS	Coauthor-Physics
ChebNet(O)	69.21 $\pm$ 0.87	75.29 $\pm$ 2.34	80.45 $\pm$ 1.09	82.64 $\pm$ 1.76	91.77 $\pm$ 0.32	90.95 $\pm$ 0.34	95.03 $\pm$ 0.11
ChebNet(M)	68.52 $\pm$ 0.86	77.38 $\pm$ 1.45	82.26 $\pm$ 0.84	85.14 $\pm$ 0.89	92.34 $\pm$ 0.41	91.54 $\pm$ 0.22	94.93 $\pm$ 0.09
$\Delta \uparrow$	-0.69	<b>+2.09</b>	<b>+1.81</b>	<b>+2.5</b>	<b>+0.57</b>	<b>+0.59</b>	-0.1
ChebNetII(O)	69.93 $\pm$ 1.15	78.42 $\pm$ 1.48	81.64 $\pm$ 0.86	84.96 $\pm$ 0.97	92.71 $\pm$ 0.46	93.08 $\pm$ 0.27	95.23 $\pm$ 0.1
ChebNetII(M)	69.54 $\pm$ 0.9	78.59 $\pm$ 1.52	81.97 $\pm$ 0.86	84.79 $\pm$ 0.83	92.58 $\pm$ 0.31	93.11 $\pm$ 0.25	95.26 $\pm$ 0.11
$\Delta \uparrow$	-0.39	<b>+0.17</b>	<b>+0.33</b>	-0.17	-0.13	<b>+0.03</b>	<b>+0.03</b>
JacobiConv(O)	70.8 $\pm$ 0.7	79.43 $\pm$ 1.45	77.15 $\pm$ 0.96	85.39 $\pm$ 0.95	92.79 $\pm$ 0.38	93.33 $\pm$ 0.23	95.32 $\pm$ 0.15
JacobiConv(M)	70.91 $\pm$ 0.66	79.65 $\pm$ 1.25	83.52 $\pm$ 0.69	84.92 $\pm$ 0.92	92.83 $\pm$ 0.36	93.27 $\pm$ 0.25	95.43 $\pm$ 0.11
$\Delta \uparrow$	<b>+0.11</b>	<b>+0.22</b>	<b>+6.37</b>	-0.47	<b>+0.04</b>	-0.06	<b>+0.11</b>
GPRGNN(O)	70.02 $\pm$ 0.7	79.24 $\pm$ 1.1	82.24 $\pm$ 0.86	84.09 $\pm$ 0.81	92.43 $\pm$ 0.24	92.99 $\pm$ 0.22	95.28 $\pm$ 0.04
GPRGNN(M)	70.4 $\pm$ 0.41	79.6 $\pm$ 0.97	82.19 $\pm$ 0.79	84.28 $\pm$ 0.86	92.53 $\pm$ 0.38	93.33 $\pm$ 0.29	95.32 $\pm$ 0.15
$\Delta \uparrow$	<b>+0.38</b>	<b>+0.36</b>	-0.05	<b>+0.19</b>	<b>+0.1</b>	<b>+0.34</b>	<b>+0.04</b>
BernNet(O)	69.12 $\pm$ 0.96	78.9 $\pm$ 1.04	81.9 $\pm$ 0.8	85.15 $\pm$ 1.14	92.63 $\pm$ 0.29	93.11 $\pm$ 0.23	95.3 $\pm$ 0.17
BernNet(M)	69.45 $\pm$ 0.64	79.07 $\pm$ 1.03	82.5 $\pm$ 0.78	85.18 $\pm$ 0.77	92.58 $\pm$ 0.36	93.07 $\pm$ 0.29	95.32 $\pm$ 0.15
$\Delta \uparrow$	<b>+0.33</b>	<b>+0.17</b>	<b>+0.6</b>	<b>+0.03</b>	-0.05	-0.04	<b>+0.02</b>

Table 3: Test accuracy of spectral GNNs with/without AdaSpec on homophilic datasets. High accuracy indicates good performance.

From Tables 2 and 3, we observe the following: (1) AdaSpec significantly improves performance on heterophilic graphs compared to homophilic graphs. There is an average accuracy improvement of 1.89% on small heterophilic graphs, an average ROC AUC improvement of 1.27% on large heterophilic graphs, and an average accuracy improvement of 0.43% on homophilic graphs. (2) AdaSpec shows greater performance improvement on small-sized graphs compared to large-sized graphs. The average node classification accuracy improvement on small graphs (Texas, Wisconsin, Cornell) is 3.45%, whereas the improvement on larger graphs (Chameleon, Squirrel) is 0.46%.

The main performance improvement stems from AdaSpec’s ability to increase node distinguishability in spectral GNNs. By refining the graph structure representation, AdaSpec enables the model to better separate nodes with similar features or structures. In homophilic graphs, low-frequency components are sufficient for smooth features, so adding more may hurt. Heterophilic graphs require richer spectral patterns, and AdaSpec help by increasing useful frequency components. In small graphs, changes in graph matrix can reveal critical structure. In large graphs, existing structure dominates, changes in graph matrix are less effective.

**Component-wise Analysis.** We report ChebNet performance augmented with AdaSpec across multiple datasets and conduct an ablation study to isolate the effects of each component. Results in Table 4 show: (1) Full components: Combining all three components consistently yields the best performance. (2) Structure-dominated graphs (e.g., Chameleon, Cora):  $\Omega_D$  outperforms  $\Omega_S$ . (3) Feature-dominated graphs (e.g., Texas, Roman\_Empire):  $\Omega_S$  outperforms  $\Omega_D$ . (4) Frequency components: Increasing non-zero frequency components via  $\Omega_F(X)$  improves performance, even when used alone. Each component within AdaSpec independently improves node distinguishability. When combined, these mechanisms complement each other, leading to the strongest overall performance.

	AdaSpec	Texas	Chameleon	Roman Empire	Amazon Ratings	Citeseer	Cora
432	ChebNet(O)	38.67	29.32	47.15	39.79	69.21	80.45
433	$\Omega_D(A)$	40.75	26.71	22.70	40.75	68.27	81.53
434	$\Omega_S(A)$	44.51	23.27	54.04	35.28	52.29	55.63
435	$\Omega_F(X)$	26.24	28.22	54.12	37.16	29.49	65.49
436	$\Omega(A, X)$	51.16	29.73	54.55	40.92	68.52	82.26

Table 4: Test accuracy of ChebNet with different components of AdaSpec across datasets that  $\Omega(A, X)$  contains all three components.

**Increased Distinct Eigenvalue Number.** We compare the number of distinct eigenvalues between the original normalized adjacency matrix  $\tilde{A}$  and the modified matrix  $\Omega_D(A)$  from AdaSpec when using ChebNet. Due to the computational cost of full eigendecomposition, we conduct this analysis on small-scale homophilic and heterophilic datasets. As shown in Table 5,  $\Omega_D(A)$  consistently increases the number of distinct eigenvalues, supporting Theorem 5.1. Standard normalized adjacency matrix  $\tilde{A}$  and its self-loop version  $\hat{A}$  are specific cases of the component  $\Omega_D(A)$  in AdaSpec by setting  $B = 0$  and  $B = 1$  respectively. We introduce richer structural information in spectral GNNs by making  $B$  learnable matrix (updated via gradient descent) in AdaSpec. The increased number of distinct eigenvalues directly enhances the model’s ability to differentiate non-isomorphic nodes.

	Dataset	Texas	Wisconsin	Chameleon	Squirrel	Cornell	Citeseer	Cora
450	$ \mathcal{V} $	183	251	890	2,223	183	3,327	2,708
451	$d_{\tilde{A}}$	113	178	845	2,213	122	2,508	2,395
452	$d_{\Omega_D(A)}$	181	229	888	2,221	144	3,227	2,645
453	$\Delta \uparrow$	68	51	43	8	22	719	250

Table 5: Number of distinct eigenvalues of the graph matrix.  $|\mathcal{V}|$  denotes the number of nodes in graphs.  $d_{\tilde{A}}$  and  $d_{\Omega_D(A)}$  are numbers of distinct eigenvalues of  $\tilde{A}$  and  $\Omega_D(A)$  in AdaSpec respectively.

**Time Complexity of AdaSpec.** We evaluate the training efficiency of ChebNet with and without AdaSpec across multiple datasets. For each dataset, we conduct ten independent runs. We report the average training time per run and the pre-computing time of  $\Psi^+(A, X)$  in Table 6. The results show that AdaSpec introduces minimal overhead and can even accelerate convergence on large heterophilic graphs (e.g., Roman\_Empire, Amazon\_Ratings). When increase graph size from Amazon\_Ratings to Coauthor-Physics, the pre-computation time rises from 0.03s to 12.44s, which is consistent with our time complexity analysis in Section 5.4. By incorporating structural and feature bias into the node representation, AdaSpec enables faster convergence and more efficient training.

Datasets	Roman_Empire	Amazon_Ratings	Tolokers	Minesweeper	Questions	Computers	Photo	Coauthor-CS	Coauthor-Physics
ChebNet (O)	1.93	1.91	1.76	1.28	2.53	4.73	3.4	3.67	4.54
ChebNet (M)	1.88	1.35	2.51	2.18	3.05	5.32	4.83	4.11	4.60
$\Delta \uparrow$	-0.05	-0.56	0.75	0.9	0.52	0.59	1.43	0.44	0.06
Pre-Computing	0.26	0.03	0.44	0.08	0.56	1.83	0.9	4.1	12.44

Table 6: Average training and pre-computing time (in seconds) for ChebNet with and without AdaSpec on large heterophilic and homophilic datasets. Pre-computing is for  $\Omega_F(X)$  in AdaSpec.

## 7 CONCLUSION AND LIMITATIONS

This work analyzes node distinguishability of spectral GNNs and shows it is governed by the interplay between the graph matrix and node features. Specifically, by the number of distinct eigenvalues and nonzero frequency components in the graph matrix’s eigenbasis. We propose AdaSpec, a plug-in module that enhances the node distinguishability of spectral GNNs, offering theoretical guarantees and empirical gains.

While effective, our approach is limited to spectral GNNs and provides only a lower bound on distinguishability. The design of AdaSpec is tailored to certain data distributions and may not generalize universally. Future work could explore more generalizable graph matrix designs, applications to dynamic graphs, and integration with advanced spectral GNNs for broader applicability.

486  
487  
**ETHICS STATEMENT**488  
489  
490  
491  
492  
493  
This work presents a theoretical analysis and algorithmic contribution to spectral GNNs for node  
classification tasks. The research does not involve human subjects, collection of personal data, or  
direct interaction with individuals. All experiments are conducted on publicly available benchmark  
datasets that have been widely used in the graph learning community. The proposed AdaSpec is  
a general-purpose technique for improving node distinguishability in spectral GNNs and does not  
target specific populations or applications that could raise fairness or discrimination concerns.494  
495  
**REPRODUCIBILITY STATEMENT**496  
497  
498  
499  
500  
501  
502  
503  
To ensure the reproducibility of our work, we have made every effort to document our methods and  
experimental setup comprehensively. The main paper provides a complete description of the proposed  
AdaSpec, including its theoretical derivation and integration with existing GNN architectures. Full  
proofs for our theoretical claims are provided in Appendix A. All experiments were conducted using  
publicly available benchmark datasets. Experimental settings, including datasets, preprocessing steps,  
model architectures, and hyperparameters, are described in detail in the main text and Appendix B.  
The complete source code, including the implementation of AdaSpec and the scripts to run all  
experiments, will be released upon acceptance, enabling full reproduction of reported results.504  
505  
506  
507  
508  
509  
510  
511  
512  
513  
514  
515  
516  
517  
518  
519  
520  
521  
522  
523  
524  
525  
526  
527  
528  
529  
530  
531  
532  
533  
534  
535  
536  
537  
538  
539

## 540 REFERENCES

541

542 Adrián Arnaiz-Rodríguez, Ahmed Begga, Francisco Escolano, and Nuria M Oliver. Diffwire:  
543 Inductive graph rewiring via the lovász bound. In *Learning on Graphs Conference*, pp. 15–1.  
544 PMLR, 2022.

545 Federico Barbero, Ameya Velingker, Amin Saberi, Michael M Bronstein, and Francesco Di Giovanni.  
546 Locality-aware graph rewiring in gnns. In *ICLR*, 2024.

547

548 Filippo Maria Bianchi, Daniele Grattarola, Lorenzo Francesco Livi, and Cesare Alippi. Graph neural  
549 networks with convolutional arma filters. *IEEE transactions on pattern analysis and machine  
550 intelligence*, 2021.

551 Hau Chan and Leman Akoglu. Optimizing network robustness by edge rewiring: a general framework.  
552 *Data Mining and Knowledge Discovery*, 30:1395–1425, 2016.

553 Eli Chien, Jianhao Peng, Pan Li, and Olgica Milenkovic. Adaptive universal generalized pagerank  
554 graph neural network. *arXiv: Learning*, 2021.

555

556 Michaël Defferrard, Xavier Bresson, and Pierre Vandergheynst. Convolutional neural networks on  
557 graphs with fast localized spectral filtering. In *NIPS*, 2016.

558

559 Yu Tang Guo and Zhewei Wei. Graph neural networks with learnable and optimal polynomial bases.  
560 *ArXiv*, abs/2302.12432, 2023. URL <https://api.semanticscholar.org/CorpusID:257205644>.

561

562 David K. Hammond, Pierre Vandergheynst, and Rémi Gribonval. Wavelets on graphs via spectral  
563 graph theory. *ArXiv*, abs/0912.3848, 2009.

564

565 Mingguo He, Zhewei Wei, Zengfeng Huang, and Hongteng Xu. Bernnet: Learning arbitrary graph  
566 spectral filters via bernstein approximation. In *Advances in Neural Information Processing Systems  
567 (NeurIPS)*, 2021.

568

569 Mingguo He, Zhewei Wei, and Ji rong Wen. Convolutional neural networks on graphs with  
570 chebyshev approximation, revisited. *ArXiv*, abs/2202.03580, 2022a. URL <https://api.semanticscholar.org/CorpusID:246652363>.

571

572 Mingguo He, Zhewei Wei, and Ji rong Wen. Convolutional neural networks on graphs with  
573 chebyshev approximation, revisited. *ArXiv*, abs/2202.03580, 2022b. URL <https://api.semanticscholar.org/CorpusID:246652363>.

574

575 Keke Huang, Yu Guang Wang, Ming Li, et al. How universal polynomial bases enhance spec-  
576 tral graph neural networks: Heterophily, over-smoothing, and over-squashing. *arXiv preprint  
577 arXiv:2405.12474*, 2024.

578

579 Ming Jin, Guangsi Shi, Yuan-Fang Li, Bo Xiong, Tian Zhou, Flora D Salim, Liang Zhao, Lingfei Wu,  
580 Qingsong Wen, and Shirui Pan. Towards expressive spectral-temporal graph neural networks for  
581 time series forecasting. *IEEE transactions on pattern analysis and machine intelligence*, 2025.

582

583 Kedar Karhadkar, Pradeep Kr Banerjee, and Guido Montufar. Fosr: First-order spectral rewiring for  
584 addressing oversquashing in gnns. In *ICLR*, 2023.

585

586 Tosio Kato. *Perturbation theory for linear operators*, volume 132. Springer Science & Business  
587 Media, 2013.

588

589 Thomas Kipf and M. Welling. Semi-supervised classification with graph convolutional networks. In  
590 *International Conference on Learning Representations*, 2017.

591

592 Ron Levie, Federico Monti, Xavier Bresson, and Michael M. Bronstein. Cayleynets: Graph con-  
593 volutional neural networks with complex rational spectral filters. *IEEE Transactions on Signal  
594 Processing*, 67:97–109, 2019.

595

596 Guoming Li, Jian Yang, and Shangsong Liang. Ergnn: Spectral graph neural network with explicitly-  
597 optimized rational graph filters. In *ICASSP 2025-2025 IEEE International Conference on Acoustics,  
598 Speech and Signal Processing (ICASSP)*, pp. 1–5. IEEE, 2025.

594 Pan Li and Jure Leskovec. The expressive power of graph neural networks. *Graph Neural Networks: Foundations, Frontiers, and Applications*, pp. 63–98, 2022.

595

596

597 Zhengpin Li and Jian Wang. Spectral graph neural networks with generalized laguerre approximation.

598 In *ICASSP 2024-2024 IEEE International Conference on Acoustics, Speech and Signal Processing* (ICASSP), pp. 7760–7764. IEEE, 2024.

599

600 Derek Lim, Joshua David Robinson, Lingxiao Zhao, Tess Smidt, Suvrit Sra, Haggai Maron, and

601 Stefanie Jegelka. Sign and basis invariant networks for spectral graph representation learning. In

602 *ICLR*, 2023.

603

604 Kangkang Lu, Yanhua Yu, Hao Fei, Xuan Li, Zixuan Yang, Zirui Guo, Meiyu Liang, Mengran Yin,

605 and Tat-Seng Chua. Improving expressive power of spectral graph neural networks with eigenvalue

606 correction. In *Proceedings of the AAAI Conference on Artificial Intelligence*, volume 38, pp.

607 14158–14166, 2024.

608

609 Hongbin Pei, Bingzhen Wei, K. Chang, Yu Lei, and Bo Yang. Geom-gcn: Geometric graph

610 convolutional networks. *ArXiv*, abs/2002.05287, 2020.

611

612 Oleg Platonov, Denis Kuznedelev, Michael Diskin, Artem Babenko, and Liudmila Prokhorenkova. A

613 critical look at the evaluation of gnns under heterophily: Are we really making progress? *arXiv preprint arXiv:2302.11640*, 2023.

614

615 Yifang Qin, Wei Ju, Yiyang Gu, Ziyue Qiao, Zhiping Xiao, and Ming Zhang. Polycf: Towards

616 optimal spectral graph filters for collaborative filtering. *ACM Transactions on Information Systems*,

617 43(4):1–28, 2025.

618

619 Yu Rong, Wenbing Huang, Tingyang Xu, and Junzhou Huang. Dropedge: Towards deep graph

620 convolutional networks on node classification. In *ICLR*, 2020.

621

622 Benedek Rozemberczki, Carl Allen, and Rik Sarkar. Multi-scale attributed node embedding. *J. Complex Networks*, 9, 2021.

623

624 Oleksandr Shchur, Maximilian Mumme, Aleksandar Bojchevski, and Stephan Günnemann. Pitfalls

625 of graph neural network evaluation. *arXiv preprint arXiv:1811.05868*, 2018.

626

627 Xu Shen, Pietro Lio, Lintao Yang, Ru Yuan, Yuyang Zhang, and Chengbin Peng. Graph rewiring

628 and preprocessing for graph neural networks based on effective resistance. *IEEE Transactions on*

629 *Knowledge and Data Engineering*, 2024.

630

631 GW Stewart. Matrix perturbation theory. *Computer Science and Scientific Computing/Academic Press, Inc*, 1990.

632

633 Jake Topping, Francesco Di Giovanni, Benjamin Paul Chamberlain, Xiaowen Dong, and Michael M

634 Bronstein. Understanding over-squashing and bottlenecks on graphs via curvature. 2022.

635

636 Xiyuan Wang and Muhan Zhang. How powerful are spectral graph neural networks. *ArXiv*,

637 abs/2205.11172, 2022.

638

639 Boris Weisfeiler and Andrei Leman. The reduction of a graph to canonical form and the algebra

640 which appears therein. *NTI, Series*, 2(9):12–16, 1968.

641

642 Keyulu Xu, Weihua Hu, Jure Leskovec, and Stefanie Jegelka. How powerful are graph neural

643 networks? In *International Conference on Learning Representations*, 2019.

644

645 Hanning Zeng, Hongkuan Zhou, Ajitesh Srivastava, Rajgopal Kannan, and Viktor K. Prasanna.

646 Graphsaint: Graph sampling based inductive learning method. *ArXiv*, abs/1907.04931, 2020.

647

648 Bingxu Zhang, Changjun Fan, Shixuan Liu, Kuihua Huang, Xiang Zhao, Jincai Huang, and Zhong

649 Liu. The expressive power of graph neural networks: A survey. *arXiv preprint arXiv:2308.08235*,

650 2023.

651

652 Jiong Zhu, Yujun Yan, Lingxiao Zhao, Mark Heimann, Leman Akoglu, and Danai Koutra. Beyond

653 homophily in graph neural networks: Current limitations and effective designs. In *Advances in*

654 *Neural Information Processing Systems*, 2020.